Nucleation and Growth of Epithelial Cell Clusters

Melanie Suaris[1], Jolie A. Breaux[2], Steven P. Zehnder[2], and Thomas E. Angelini[2]

[1]*J. Crayton Pruitt Family Department of Biomedical Engineering, College of Engineering, University of Florida JG-56 Biomedical Sciences Building, Box 116131, Gainesville, Florida,USA 32611-6131*

[2]*Department of Mechanical and Aerospace Engineering, College of Engineering, University of Florida 124-MAE-C Gale Lemerand Drive, Gainesville, Florida, USA 32611-6131*

Abstract. Throughout many processes in tissues, large groups of cells move either in dispersed populations or in condensed populations. Very often each type of motion involves a transition between dispersed and condensed phases. Here we study a transition in cell migration as a cell population changes from sparse to dense. We observe a process that resembles homogeneous nucleation in other classical phase-segregating systems, as well as a diverging correlation length that scales with reduced cell density to the ½ power.

Keywords: cell migration, cell mechanics, collective migration, cell cohesion
PACS: 87.17.Rt, 87.18.Ed, 87.18.Gh

INTRODUCTION

Cell migration is an essential part of tissue development, function, and disease. Cells move collectively in condensed groups during several major stages of embryonic growth, during the re-epithelialization process in wound healing, and during some types of cancer metastasis[1-4]. By contrast, large populations of cells move as individuals during the very same stages of life in tissues. In healthy tissue for example, fibroblasts migrate through a sparsely populated extracellular matrix that constitutes connective tissue[5,6]. In an injury, during the inflammation and proliferation phases of wound healing, many cell types migrate in and out of the wound, while granulation tissue is produced by fibroblasts and condensed groups of endothelial cells grow[7,8]. In the epithelial-to-mesenchymal transitions (EMTs) during development and in cancer, condensed groups of cells become detached from one another and disperse, migrating as individuals[9]. Thus, the many types of cell motility in tissues involve migration within dispersed populations, condensed populations, and transitions between dispersed and condensed populations. Current understanding of collective migration has been achieved mostly from the study of cell motion in confluent monolayers or from sheet migration studies in "scratch test" would-healing assays[10-14]; the transition between dispersed and condensed phases has been studied far less than the condensed phase alone[15]. Deeper and broader knowledge of the transition between cell migration in a dispersed population and cell migration in a condensed population will greatly improve our understanding of these less-understood cell migration processes that are so important to tissues.

Here we study the density dependent motion of cells as they populate a surface. We start with a sub-confluent cell population and observe collective cell motion as the layer transitions from a dispersed distribution to a highly condensed monolayer. We find several basic similarities between this cell migration transition and a gas-to-liquid phase transition. As cell density rises, migration velocity drops, and the slower cells form dense clusters. By measuring the size and lifetimes of the clusters, we find a critical cluster size, below which clusters break up and above which clusters grow steadily to become part of a macroscopic condensed phase. The cluster size diverges with increasing cell density, and the migration velocity decreases in a divergent manner with increasing cell density, allowing the measurement of critical exponents associated with this transition.

RESULTS

Cell Clustering and Migration Speed

To study the transition between cell migration in a dispersed population and migration in a condensed population, we measure cell density and migration velocity over time. Cells are sparsely plated in a

4th International Symposium on Slow Dynamics in Complex Systems
AIP Conf. Proc. 1518, 536-540 (2013); doi: 10.1063/1.4794630

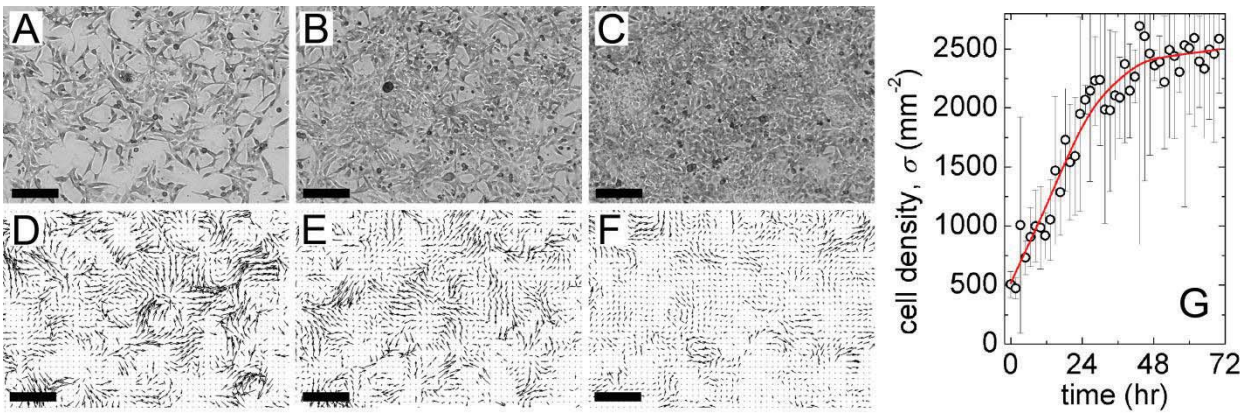

FIGURE 1. Cells are sparsely deposited on a cell culture surface and observed over time. At early times, cells are large and there is a great deal of unoccupied area (A). At later times, cell size is reduced and the free space begins to fill in (B) until, ultimately, the entire area is covered and the cells become small and tightly packed (C). Correspondingly, migration speeds are high and spatially heterogeneous at the lowest densities (D), and as the cell layer fills in, dense clusters form which move more slowly than cells in low-density areas (E). At the highest densities, the average migration speed has dropped significantly and the slow homogeneous patches have grown in size (F). We measure cell density over time by manually counting cells at select time points. A smooth spline is drawn through the data-points to estimate cell density at all times (G). (Scalebars = 200 μm)

collagen coated, glass-bottomed culture dish and observed in an environmentally controlled chamber on microscope a stage. Time lapse imaging is performed for approximately three days, during which cells migrate, proliferate, and condense into a confluent layer. Cell density is measured by manually counting cells at selected time-points, and migration velocity fields are measured with image analysis software (see Materials and Methods). By comparing the velocity fields to the cell layer images, we directly observe that smaller cells within condensed clusters move more slowly than larger cells near regions devoid of cells. Over the course of the experiment, the average cell density increases 5-fold, as shown in Figure 1.

Across length-scales of order 1 millimeter, cell migration velocity fields are spatially heterogeneous, exhibiting smaller patches that appear homogeneous in magnitude and direction over the shorter length-scales, in the range of 100's of microns. Over the entire 1.6mm x 2.1mm field of view, we explore the distribution of local migration speeds by computing histograms of velocity vector magnitudes. At each time point a histogram curve, $n(v)$, is computed with a uniform bin-size and normalized such that $n(v)$ equals the percentage of velocity vectors with magnitudes that fall within a bin centered at the speed, v. Examination of all histograms over time, arranged into a 2D intensity map, reveals a steady decrease in migration speed and a steady sharpening of the distribution. Selected time points show this shift of the histogram peak to lower speeds and the narrowing of the distributions, as well as a substantial tail on the high speed side of the distributions (Figs. 2A and 2B).

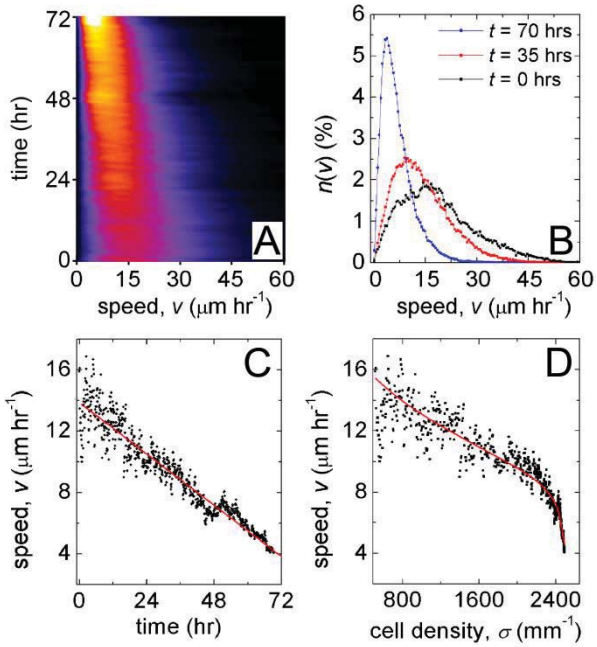

FIGURE 2. We measure a speed histogram, $n(v)$, at every time point during the experiment. A false-color intensity map of all histograms shows a peak that narrows and shifts to lower speeds as time progresses (A). The histograms are normalized so that each point of $n(v)$ equals the percentage of speeds in bin v, with a bin-size equal to 0.46 μm hr^{-1} (B). The speed decreases monotonically in time (C), but dramatically turns downward with increasing cell density, as cell density begins to approach an upper limit (D).

To determine a characteristic speed in the system at each time point, we find the speed corresponding to

the peak in each $n(v)$, rather than compute the arithmetic mean speed. This approach is frequently used to analyze strongly asymmetric distributions, and reduces the influence of the smaller population of higher magnitude velocity vectors. The result of this process reveals an average migration speed decreasing linearly in time, from approximately 14 μm hr^{-1} to 4 μm hr^{-1}. The speed exhibits a strongly nonlinear dependence upon cell density. As cell density exceeds approximately 2000 cells mm^{-2}, the migration velocity turns downward in a dramatic, divergent fashion (Fig. 2D).

Cluster Nucleation and Growth

At the highest cell density measured, the entire boundary of each cell is in contact with neighboring cells, and cells are round in cross-sectional shape with a reduced cross-sectional area, relative to unconfined cells. Accompanying this apparent increase in structural homogeneity, the velocity field becomes more homogeneous, as indicated by the substantially narrowed distribution of speeds. We therefore employ a dynamic criterion to separate the cell layer into two populations; at the highest density, cells covering 90% of the surface move more slowly than 15.5 μm hr^{-1}, which we choose to be a cutoff speed. We take the magnitude of each velocity vector to create 2D speed maps, applying this cutoff criterion and grouping regions into two populations: slow-moving clusters and fast moving dispersed regions. Binary, segmented speed maps are created and cluster sizes are measured over time. At low cell densities, clusters are small and sparse; approximately 10% of the surface is covered by clusters. As density rises, the number of clusters rises and the fraction of surface area covered rises until the highest density is reached, at which time 90% of the surface is covered by clustered cells. (Fig. 3 A-C).

We study the growth and dispersal of clusters by creating a three dimensional stack from the binary, segmented speed maps, identifying regions connected in space and time. Many clusters exist only for a short time, and other clusters persist permanently, eventually becoming part of the macroscopic condensed phase. A comparison between the sizes of short lived clusters and permanent clusters shows that there is a critical nucleus size for cluster growth. Clusters below approximately 5000μm^2 are not stable and are short lived. This critical nucleus size corresponds to a cluster of approximately ten cells. Intriguingly, the average cluster size scales with the migration speed, approximately, to the -0.2 power (Fig. 3 D, E).

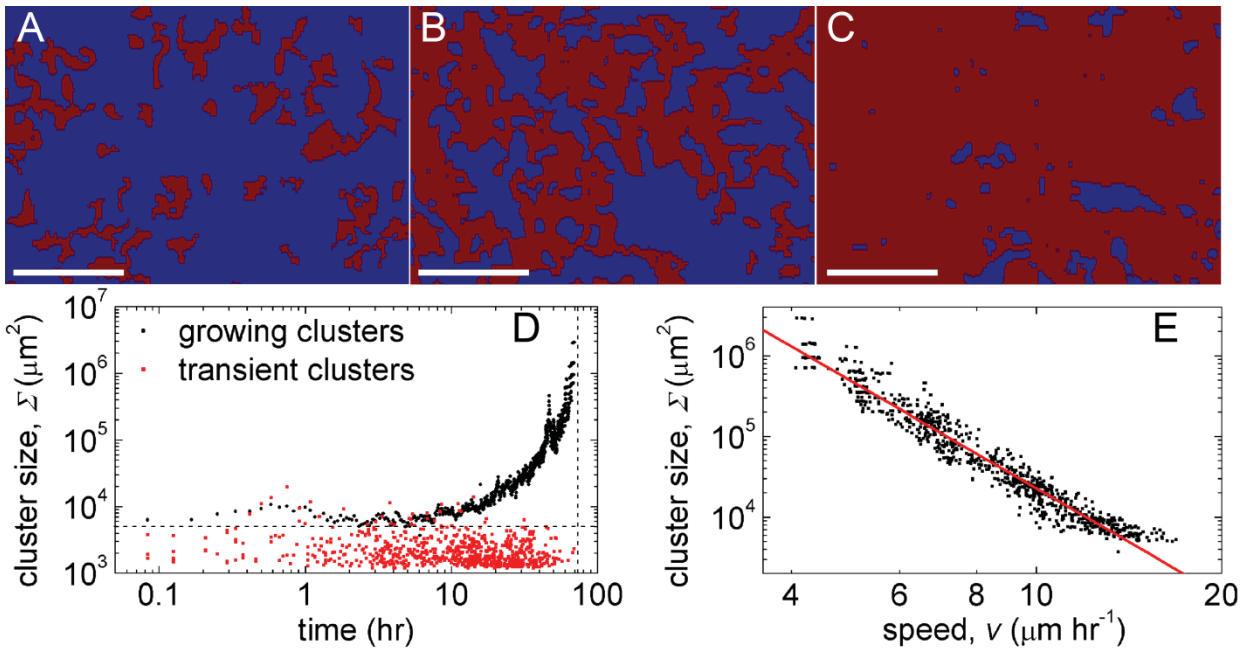

FIGURE 3. Small, transient clusters of slow moving cells cover approximately 10% of the surface at the lowest cell densities (A). As cell density rises, the number of clusters grow and several large clusters are established that eventually grow to fill most of the surface (B,C). An analysis of the size and lifetime of the clusters allows the separation of transient clusters and growing clusters. Average cluster sizes versus time show that there is a critical cluster size of approximately 5000 μm^2 (D). Cluster size scales with speed as a power-law with an approximate exponent of -0.2 (E). (Scalebars = 330 μm)

Scaling In Cluster Size and Migration Speed

The power law relationship between cluster size and migration speed, and the apparent divergences in Σ and v as density rises over time, suggest that both parameters may follow critical scaling laws as a function of density. In analogy to colloidal phase transitions, previous observations of the density dependent behavior of cell monolayers show that cell density plays a role inverse to that of temperature in atomic and molecular phase transitions[10]. Thus, to explore critical behavior associated with cluster size and migration speed, we carry out a scaling analysis as a function of cell density. We define a reduced density as

$$\tilde{\sigma} = \frac{\sigma_{cr} - \sigma}{\sigma_{cr}},$$

where σ_{cr} is the critical density, and we fit the cluster size data with a scaling law, $\Sigma = \Sigma^* \tilde{\sigma}^{-p_1}$. We find a critical density of σ_{cr} = 2499 ± 9 mm^{-2}, a critical amplitude Σ^* = 4370 +- 460 mm^2, and a critical exponent of p_1 = 1.01 ± 0.02. We perform a similar analysis on the migration speed data, fitting the critical scaling law, $v = v^* \tilde{\sigma}^{p_2}$. We find nearly the same critical density, σ_{cr} = 2507 ± 3 mm^{-2}, a critical amplitude of v^* = 14.17 ±0.07 μm hr^{-1}, and a critical exponent, p_2 = 0.214 ± 0.002. The power law scaling in for both Σ and v is directly seen by re-plotting the data versus reduced density, as shown in Figure 4.

The critical density observed here is very close to the glass-transition density previously observed in a confluent cell sheet[10]. We believe the significance of this density in both types of transition is that there is a lower limit on cell size, and therefore an upper limit on cell density. We take note that the cluster size critical amplitude, Σ^*, is very close to the critical nucleus size estimated directly from cluster lifetime measurements. Likewise, v^* is very close to the migration speeds at the lowest density, where most clusters are below the critical cluster size. Despite the lack of a theoretical model particular to cell migration to describe the physical driving forces that control this transition and predict the critical amplitudes, we may gain insight from the critical exponents. For example, the scaling of cluster size with $\tilde{\sigma}^{-1}$ means that there is a growing correlation length, $\xi = \xi^* \tilde{\sigma}^{-1/2}$. This suggests that the transition observed here may fall within the mean-field universality class, similar to a gas-liquid phase transition.

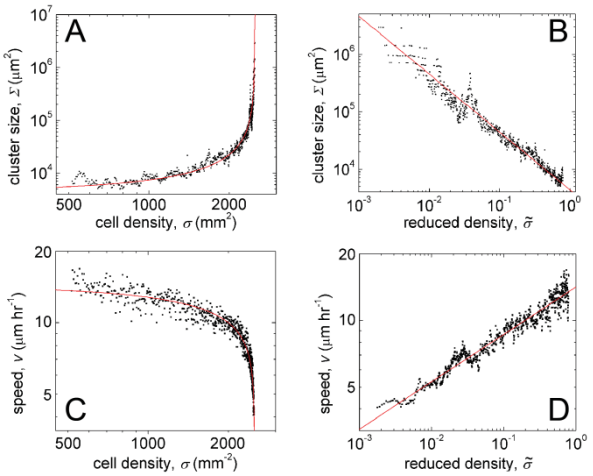

FIGURE 4. Cluster size exhibits a divergent-like increase with increasing cell density (A), which scales like a power-law when plotted versus reduced density (B). The speed also shows divergent-like behavior with increasing density (C) and grows as a power-law with increasing reduced density (D).

DISCUSSION AND CONCLUSIONS

Here we explore cell migration during a transition between a low-density, dispersed cell population and a high-density condensed population. We find that transient, slow moving clusters of cells nucleate and disperse over time, and above a critical nucleus size, clusters persist indefinitely, eventually merging to form a macroscopic condensed phase. This process is reminiscent of homogeneous nucleation in classical phase segregation. If there is a free energy cost associated with creating an interface between a condensed phase and a dispersed phase, but there is a free energy benefit for assembling the cohesive cells, a critical nucleus size can be predicted by minimizing

$$\Delta F = 2\pi R\gamma - \pi R^2 \varepsilon,$$

where γ is a line tension generated by cell-cell cohesion, and ε is the free energy per unit area gained for transferring a cell into the condensed phase. The minimum of this function defines the critical nucleus size, $R_c = \gamma/\varepsilon$. The cohesive energy associated with cadherin junctions has been studied extensively[16]; a typical value of this energy density is 3 mJ m^{-2}, and the height of the cell-cell interface in an MDCK layer is approximately 6 μm. We estimate γ from the product of the energy density and the cell height, finding about 0.02 μN. From the observed cutoff between transient and permanent clusters, we find $R_c \approx 70$ μm, and then estimate ε to be 0.3 mJ m^{-2}, or about one tenth of the cohesive energy density. We note that the surface tension of finite-sized 2D cell clusters has been measured recently [17], however the energy density

change associated with condensing isolated cells into clusters has never before been observed.

Since the average cell density is continually rising in this system, it is important to consider whether the growing correlation length may be observed because density fluctuations do not have sufficient time to relax. Since cell divisions generate local density fluctuations, we compare the time it takes a cell to migrate its own body-length to the time between cell divisions. At the highest densities, cells are approximately 20 μm across, migrating at 4 μm hr^{-1}. The corresponding migration time is 5 hours. At the lowest densities, the same migration time is less than 2 hours. In previous work we directly measured the division time in MDCK monolayers, finding a division time of approximately 40 hours. So, even if a cell is surrounded by 6 neighbors, it can migrate its own body length before it divides and before any of its neighbors divide. Thus, density fluctuations relax quickly enough, compared to the rate of density rise, that the growing correlation length is not likely to be a dominantly kinetic effect.

The transition observed here may have several implications in tissue engineering applications, in which extra-cellular matrix (ECM) based scaffolds are sparsely seeded with cells and grown in bioreactors. If a tissue growth strategy depends on cell migration and proliferation, both the final state of the system and the rate at which the system reaches maturity may be strongly influenced by both the critical nucleus size and by the critical cell density, observed here. Likewise, critical cluster size and critical density may play significant roles in any application involving micro-patterning of surfaces to control cell distribution, migration, and adhesion.

MATERIALS AND METHODS

Cell Culture and Sample Preparation

MDCK II cells are cultured in DMEM with 5% Fetal Bovine Serum (FBS) and 1% Penicillin Streptomycin (Pen-Strep). A 1.5 μl drop with 500 cells is deposited at the center of a glass bottom collagen coated culture dish and stored at room temperature for 20 minutes. The dish is then filled with cell culture media and relocated to an incubator where it is maintained at 37 C with 5% CO_2. After two hours, the sample is brought to a temperature controlled microscope stage where conditions remain at 37 C and 5% CO2.

Bright Field Microscopy and Image Analysis

The cell island is imaged in bright field and two separate images per minute are taken at the center of the island. One in-focus image is taken to measure migration velocity fields and one out-of-focus image is used to distinguish cell clusters from empty regions. Velocity fields are computed using particle image velocimetry (PIV) methods previously reported[11]. At the end of each 200 minute interval, cell density is estimated by manually counting the number of cells within randomly chosen regions in the image. Regions devoid of cells are identified by applying an edge-finding algorithm to the out-of-focus images; the contrast between cells and empty regions is greatly enhanced by imaging at a focal plane above the cells.

ACKNOWLEDGMENTS

This work was supported by The University of Florida Division of Sponsored Research Opportunity Fund, grant number GM03038.

REFERENCES

1. Martin,P. , Parkhurst, S., *Development* **131**, 3021-3034 (2004).
2. Friedl,P. , Hegerfeldt, Y. , Tusch, M., *The International Journal of Developmental Biology* **48**, 441-449 (2004).
3. Friedl,P., *Current Opinion in Cell Biology* **16**, 14-23 (2004).
4. Lecaudey, V., Gilmour, D., *Current Opinion in Cell Biology* **18**, 102-107 (2006).
5. Even-Ram, S., Yamada, K.M., *Current Opinion in Cell Biology,* **17**, 524-532 (2005).
6. Langevin, H.M., Cornbrooks, C.J., Taatjes, D.J., *Histochemistry and Cell Biology*, **122**, 7-15 (2004).
7. Grinnell, F., *The Journal of Cell Biology*, **124**, 401-404 (1994)
8. Witte, M.B., Barbul, A., *Surgical Clinics of North America*, **77**, 509-528 (1997).
9. Thiery, J. P, *Current Opinion in Cell Biology* **15**, 740-746 (2003).
10. Angelini, T.E et al., *PNAS* **108**, 4714-4719 (2011).
11. Angelini, T.E , Hannezo, E., Trepat, X., Fredberg, J., Weitz, D., *Physical Review Letters* **104**, 168104 (2010).
12. Trepat, X. et al., *Nature Physics* **5**, 426-430 (2009).
13. Farooqui, R., Fenteany, G., *Journal of Cell Science* **118**, 51-63 (2004).
14. Nnetu, K.D., Knorr, M., Strehle, D., Zink, M., Kas, J.A., *Soft Matter*, **8**, 6913-6921 (2012).
15. Szabo, B. et al., *Physical Review E* **74**, 061908 (2006).
16. Foty,R., Steinberg, M., *Developmental Biology* **278**, 255-263 (2004).
17. Mertz, A.F., Banerjee, S., Che, Y., German, G.K., Xu, Y., Hyland, C., Marchetti, M.C., Horsley, V., Dufresne, E.R., *Physical Review Letters*, **108**, 2012.